INTERNATIONAL JOURNAL FOR NUMERICAL METHODS IN FLUIDS
Int. J. Numer. Meth. Fluids 2007; **53**:561–571
Published online 24 July 2006 in Wiley InterScience (www.interscience.wiley.com). DOI: 10.1002/fld.1294

A numerical simulation on diffuser-nozzle based piezoelectric micropumps with two different numerical models

Jin Jeong[1] and Chang Nyung Kim[2, 3, *, †]

[1]*Department of Mechanical Engineering, Kyung Hee University, Korea*
[2]*College of Advanced Technology, Kyung Hee University, Korea*
[3]*Industrial Liaison Research Institute, Kyung Hee University, Korea*

SUMMARY

This study has been conducted to compare two different numerical models for the evaluation of the performance characteristics of a diffuser-nozzle based piezoelectric micropump. Here, the transient displacements of the membrane and the flow characteristics in the piezoelectric micropump have been closely investigated with the FSI model and the prescribed deformation model for two different frequencies. It has been found that the behaviour of the membrane computed with the FSI model is not in accordance with that with the prescribed deformation model, and that the net flow rate with the FSI model is larger than that with the prescribed deformation model. Therefore, the choice of numerical model is very important in conducting numerical analysis for piezoelectric micropumps. The results of this study can be utilized as basic data for the design and analysis of piezoelectric micropumps. Copyright © 2006 John Wiley & Sons, Ltd.

Received 13 November 2005; Revised 27 April 2006; Accepted 30 April 2006

KEY WORDS: piezoelectric micropump; diffuser-nozzle; fluid–structure interaction; numerical analysis

1. INTRODUCTION

Various micro-systems have been recently focused with the development of micro-electro mechanical system (MEMS) and micro-machining technology. Especially, the technology on the micro-fluidic device has been rapidly developed with the advance of micro-systems. These

*Correspondence to: Chang Nyung Kim, College of Advanced Technology, Kyung Hee University, 1 Seochon, Kihung, Yongin, Kyunggi 449-701, Korea.
†E-mail: cnkim@khu.ac.kr

Contract/grant sponsor: Korea Research Foundation; contract/grant number: KRF-2004-041-D00119

micro-fluidic devices for controlling infinitesimal flow rate can be applied in many fields such as biology, chemistry, medical science, biomedical engineering, etc. [1].

Micropumps, essential parts of micro-fluidic devices, are in need of high-end technology including the design of micro-systems, the micro-machining, and the micro-fluid mechanics. Based on the actuation method, micropumps can be classified into various types such as electrostatic micropump, piezoelectric micropump, electro-hydro-dynamic (EHD) micropump, thermopneumatic micropump, electroosmotic micropump, etc. The diffuser-nozzle-based piezoelectric micropump induces the motion of membrane using the piezoelectric effect of the piezo materials, and gets pumping effect yielded by the difference in the flow resistance between the diffuser and the nozzle. The piezoelectric micropump has merits in the sense that the structure is simple and the displacement of the membrane is relatively large [2]. These features of the piezoelectric micropumps have not been investigated deeply because of the lack of high accurate instruments and the difficulties of measurements in the process of experiments. Therefore, various studies on the characteristics of piezoelectric micropumps have been lively conducted these days by many researchers.

Stemme and Stemme [3] manufactured and tested valveless micropumps with diffuser and nozzle and compared it with the same sized micropump with passive check valves. Schulte *et al.* [4] presented a modular solution approach for simulation of coupled problem such as fluid–structure interaction problem which can be observed in a micropump and conducted a simple test to verify the method. They called their solution method a quasi-stationary simulation because of the limitation in the interaction method, asserting the introduction of fully transient simulation method. Olsson *et al.* [5] manufactured valveless micropump using deep reactive ion etching (DRIE) method and investigated the influence of the shape associated with the width of throat, the length of diffuser and nozzle, and the divergence angle of diffuser/nozzle on the flow characteristics and performance of diffuser-nozzle based micropump. Anderson *et al.* [6] evaluated the influence of the density and viscosity on the pumping characteristics using experimental method and observed the flow characteristics in the chamber. Nguyen and Huang [7, 8] manufactured valveless miniature pump with printed circuit board (PCB) and measured the displacement of the membrane covering the protuberance and the rim of the non-plate type piezo disk. Also, they compared the experimental results with the numerical results obtained by assuming that the deforming curve of the membrane follows Timoshenko's theory [9]. Song [10] numerically evaluated the displacement of the membrane assuming the deforming curve of the membrane to be a part of the circle and compared his results with experimental data.

These previous studies have been mainly conducted through experimentation, measuring the flow rate and the displacement of membrane, and some numerical studies have analysed only fluid region two dimensionally assuming the displacement of the membrane. As mentioned before, some numerical studies using the FSI model have been conducted only with quasi-stationary simulation method, not with fully transient simulation method.

However, a fully transient numerical analysis considering the interaction between fluid and structure is necessary to correctly evaluate the performance of the piezoelectric micropump because the piezo disk and the working fluid interact each other. In this study, the performance characteristics for the diffuser-nozzle-based piezoelectric micropump have been evaluated two dimensionally with fully transient fluid–structure interaction (FSI) model, and have been compared with those of the prescribed deformation model. Also, to investigate the effect of the change of frequencies, the flow characteristics and the dynamic characteristics of the membrane in the frequencies of 50 and 90 Hz have been analysed. Here, in the FSI model the membrane motion has been computed with the

DOI: 10.1002/fld

piezoelectric effect of the piezo disk while in the prescribed deformation model the membrane deformation has been prescribed based on the result of the FSI model.

2. NUMERICAL ANALYSIS

2.1. Numerical model

A piezoelectric micropump can be made of plate type piezo disk as shown in Figure 1. A transient numerical analysis for the diffuser-nozzle based piezoelectric micropump has been conducted with the FSI model and prescribed deformation model. The working fluid is sucked and pushed by the membrane which is stuck on the upper surface of the piezo disk of the micropump.

As depicted in Figure 1, the diffuser-nozzle-based piezoelectric micropump consists of the chamber (with the diameter of 20 mm, and the height of 200 μm), the diffuser and nozzle (with the divergence angle of 7°), and the piezo disk (with the diameter of 20 mm and the height of 5 mm). The piezo disk is made of the pic 153 materials, manufactured by PI Co. Ltd. and the specific properties of the piezo disk are presented in Table I. The analysis has been conducted with frequencies of 50 and 90 Hz in each model.

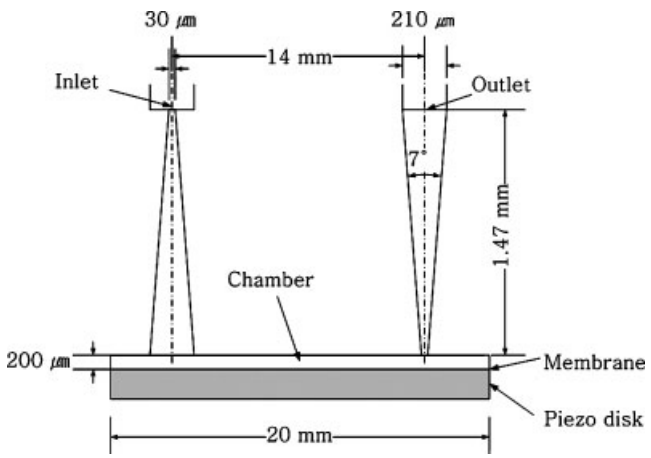

Figure 1. Schematic diagram of the diffuser-nozzle-based piezoelectric micropump.

Table I. Properties of the piezo disk (pic 153).

Density (kg/m^3)	7750
Relative permittivity	4500
Resistivity (Ωm)	105
Charge constants d_{33} ($\times 10^{-12}$ m/V)	750
Voltage constants g_{33} ($\times 10^{-3}$ Vm/N)	18
Young's modulus ($\times 10^{10}$ N/m^2)	4.5

DOI: 10.1002/fld

2.2. Numerical method

2.2.1. FSI Model. To investigate minutely the characteristics of the piezoelectric micropump it is necessary to calculate the effect of the interaction between the fluid flow and the behaviour of piezo disk (the structure). The governing equations for fluid flow are the continuity equation and the Navier–Stokes equation, which can be written in a strong conservation form in the curvilinear coordinates as follows:

$$\frac{\partial}{\partial t}\left(\frac{\rho}{J}\right)+\frac{\partial}{\partial \xi^j}\left(\frac{\rho U_j}{J}\right)=0 \tag{1}$$

$$\frac{\partial}{\partial t}\left(\frac{\rho u_i}{J}\right)+\frac{\partial}{\partial \xi^j}\left(\frac{\rho U_j u_i}{J}\right) =-\frac{1}{J}\frac{\partial \xi^j}{\partial x_i}\frac{\partial p}{\partial \xi^j}+\frac{\partial}{\partial \xi^k}\left[\frac{\mu}{J}\frac{\partial \xi^k}{\partial x_j}\left(\frac{\partial \xi^l}{\partial x_j}\frac{\partial u_i}{\partial \xi^l}+\frac{\partial \xi^l}{\partial x_i}\frac{\partial u_j}{\partial \xi^l}-\frac{2}{3}\delta_{ij}\frac{\partial u_l}{\partial \xi^m}\frac{\partial \xi^m}{\partial x_l}\right)\right] \tag{2}$$

where ρ is the fluid density, μ the effective dynamic viscosity, u_i the Cartesian velocity component, p the pressure, t the time, x_i the Cartesian coordinate, U_j the velocity component in the ξ^j direction (contravariant velocity component), and J the coordinate transformation Jacobian. Also, the governing equation for piezoelectric effect of the piezo disk can be generally written in forms as follows:

$$\{\sigma\}=[S]\{\gamma\}-[a]\{E\} \tag{3}$$

$$\{D\}=[a]^{\mathrm{T}}\{\gamma\}+[e]\{E\} \tag{4}$$

where $\{\sigma\}$ is the stress vector, $[S]$ the stiffness matrix, $\{\gamma\}$ the strain vector, $[a]$ piezoelectric coupling matrix, $\{E\}$ the electric field vector, $\{D\}$ the electric flux density vector, and $[e]$ the dielectric matrix.

Here, the effect of the motion of the piezo disk is transmitted to the fluid region only through the grid velocity term of the equations for fluid flow at the fluid–structure interface because the fluid velocity is always equal to the surface velocity of the structure at the fluid–structure interface, and there is no direct coupling between the flow equations and the structure equation. The fluid dynamics solver, structural dynamics solver (for piezoelectric effect) and the fluid–structure interaction solver are embedded in the calculation process.

In the process of numerical calculation of fluid domain the fluid velocities and pressures are computed with the continuity equation and the Navier–Stokes equation at every time step. In the process of numerical calculation of structure domain the piezoelectric force and the pressure acting on the piezo disk by the fluid in the chamber are used to evaluate the displacement of the piezo disk at a given iterative calculation step. Also, the velocity of the surface of the piezo disk (that is, the membrane) is imposed on the fluid in the chamber, yielding the altered flow domains in the next iterative calculation, which means that the fluid and the structure are interacting. The fluid velocities and pressure are again computed in the altered domain and the updated fluid forces on the piezo disk are applied as boundary conditions of the motion of the structure. Then the grid distribution is reconstructed based on the deformed domains of the fluids and the structure at

DOI: 10.1002/fld

this iterative calculation step. This iterative calculation continues until both the flow and structure variables converge. The numerical calculation proceeds, again, to the next time step and then the above procedure is repeated. The flow chart of the numerical calculation process with FSI model is shown in Figure 2.

In this study, the input voltage at the bottom of the piezo disk is of the rectified sine wave ranging from the minimum −500 to 0 V while the input voltage at the top of the piezo disk is 0 V.

2.2.2. Prescribed deformation model. In the prescribed deformation model, the displacement of membrane is given with Equation (5) that is expressed as a function of the distance (x) and time (t), following the Timoshenko's theory [9]:

$$\mathrm{d}y(x,t) = A(t)\left\{1-\left(\frac{x}{X}\right)^2\right\}^2 \tag{5a}$$

$$\begin{aligned} A(t) &= A_0 \sin(2\pi f t) \quad \left(\text{for } 0 \leqslant t \leqslant \frac{1}{2f}\right) \\ &= 0 \qquad\qquad\quad \left(\text{for } \frac{1}{2f} < t \leqslant \frac{1}{f}\right) \end{aligned} \tag{5b}$$

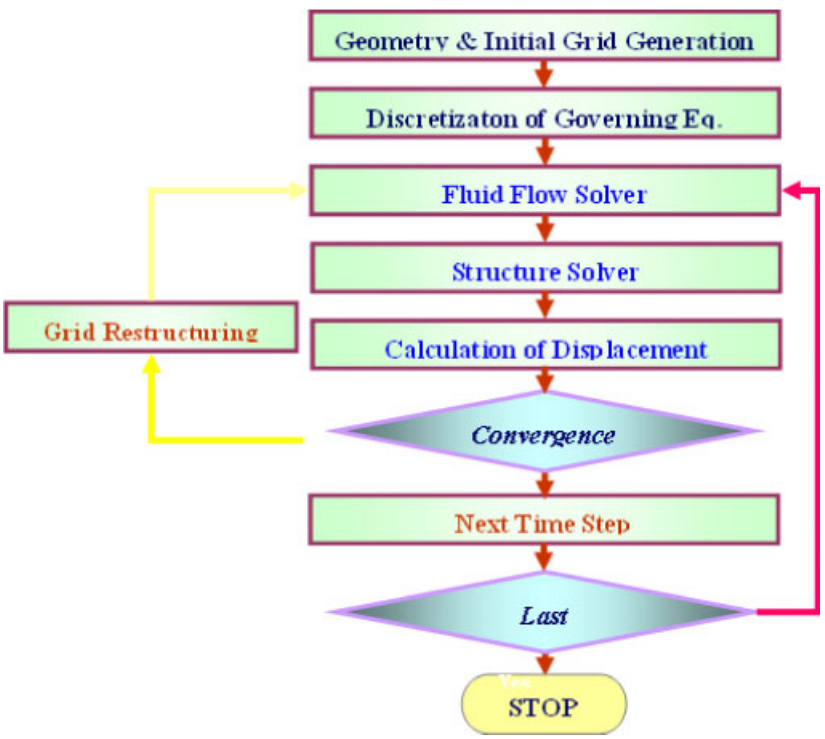

Figure 2. The flow chart of the calculation process with the FSI model.

DOI: 10.1002/fld

where x is the distance from the centre, X the half width of the chamber, f the frequency of the piezo disk and A_0 the maximum displacement at the centre of the piezo disk in a cycle. Here, $A(t)$ is of the sine wave resembling the rectified input voltage.

The displacement of the membrane given by Equation (5) is applied to the fluid–structure interface. And then the continuity equation and the Navier–stokes equation in the fluid region are calculated with time.

3. DISCUSSION

In the numerical calculation of the current problem formulation, several grid systems have been under consideration. For the FSI model and prescribed deformation model various grid systems have been used with many different time steps under consideration, and their results have been compared. The above work has led us to use grid system in the current calculation with about 20 000 structured grids (about 15 000 structured grids in the fluid domain).

Search for proper time step size has been one of the difficulties in the current calculation. At first, an effort to find out some variable time step size has been carried out in association with the fact that a smaller time step is required when the membrane and the water are moving fast while somewhat larger time step can be allowable when the membrane and water is moving slowly or is not moving. However, this type of trial to find out some proper variable time step size turned out to be meaningless in the current calculation. To find out suitable fixed time step size for a whole time domain, many different time steps have been tried and their results have been compared, which has led us to adopt $\Delta t = 0.0002$ s in the calculation with 50 Hz and $\Delta t = 0.0001$ s with 90 Hz.

Also, the first-order upwind scheme is used for the discretization scheme of convection and diffusion terms in the fluid domain to avoid lengthy calculation time. It takes about 12 h to compute unsteady pumping for two cycles with Pentium-4 3.2 GHz PC. And, if the dimensionless residuals in all grid points are less than 10^{-4}, the calculation is assumed to be converged. The numerical analysis has been conducted with CFD-ACE 2004.

3.1. Dynamic characteristics of the piezo disk

To investigate the dynamic characteristics of the piezo disk, the displacements of the piezo disk have been computed with Equations (3) and (4) for the FSI model, and with Equation (5) for the prescribed deformation model. As shown in Figure 3, the maximum displacement of the piezo disk in each model has been obtained at the centre point of the membrane. Here, the deformation of the piezo disk in the FSI model indicates that the central part is almost flat, while that in the prescribed deformation model shows that the displacement is of smooth curves.

As depicted in Figure 4, the central displacement of the piezo disk with time has been obtained. Here, the behaviour characteristics of the piezo disk in the FSI model is almost similar to that in the prescribed deformation model with both 50 and 90 Hz, and the maximum displacements of the piezo disk are about 60 μm in the two cases. However, the deformation of the piezo disk in the FSI model starts a little bit later than that in the prescribed deformation model as can be seen when t is almost zero. The behaviour of the piezo disk in the FSI model is very closely related to that of the rectified input voltage which has the time delay compared with the applied voltage. However, as shown in Figure 5, as the time goes on the position of the membrane in the FSI model chases, and

DOI: 10.1002/fld

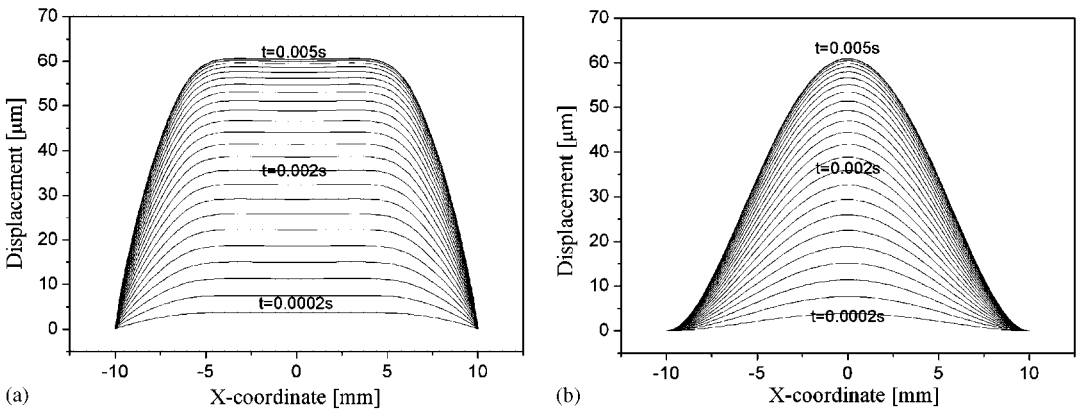

Figure 3. Displacement of the two different piezo disks ($f = 50$ Hz): (a) FSI model; and (b) prescribed deformation model.

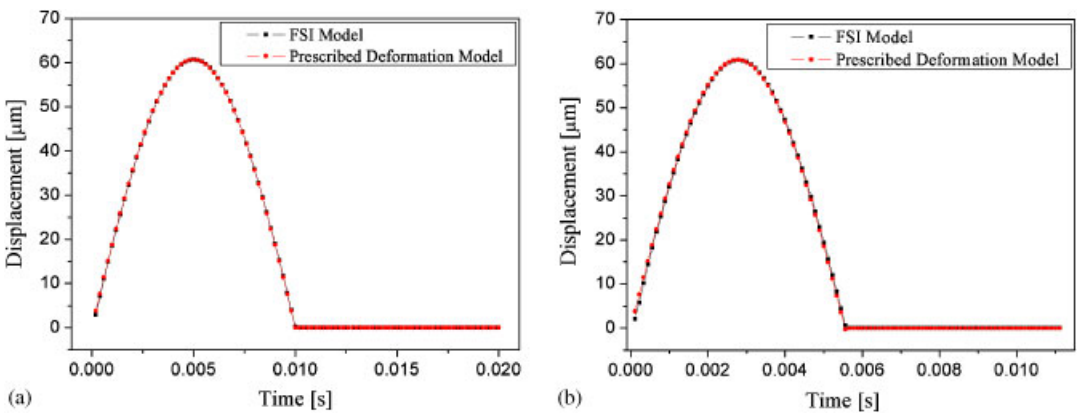

Figure 4. The central displacements of the piezo disk with time: (a) 50 Hz; and (b) 90 Hz.

around at the time of one-fourth cycle pass over the position in the prescribed deformation model in the ascending period. The maximum difference between the two displacements at the centre of the membrane in the FSI model and prescribed deformation model is observed in the very beginning part of the ascending period with both 50 and 90 Hz and the maximum difference with 90 is larger than that with 50 Hz.

As explained before, the prescribed deformation model includes the assumption that the behaviour of the membrane is of the same pattern as that of the input voltage which has a form of a sine function. Therefore, the prescribed deformation model can only simulate approximately the behaviour of the membrane in the micropump.

DOI: 10.1002/fld

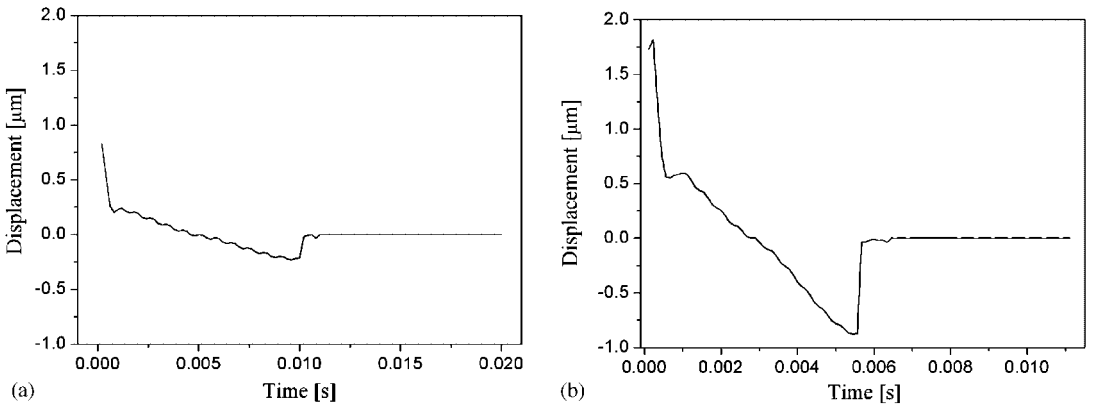

Figure 5. Differences between the two central displacements with time: (a) 50 Hz; and (b) 90 Hz.

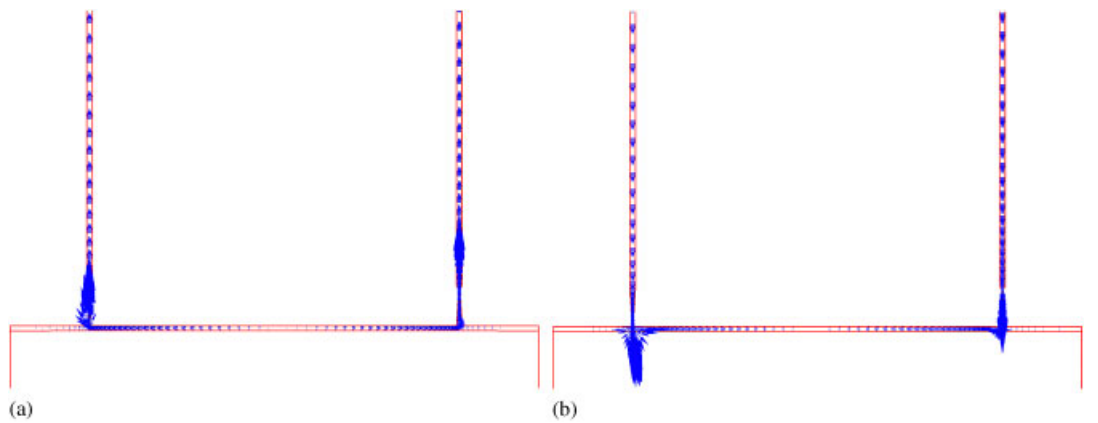

Figure 6. Velocity vectors in the piezoelectric micropump in the FSI model with $f = 50$ Hz: (a) $t = 0.001$ s; and (b) $t = 0.009$ s.

3.2. *Flow characteristics with different numerical models*

To investigate the flow characteristics in the chamber, velocity distributions and flow rates with time at the inlet and outlet have been computed with FSI model and prescribed deformation model for two cycles in both 50 and 90 Hz. The obtained velocity vectors have been depicted in Figure 6. It has been found that the fluid flows out both at the inlet and outlet in the ascending period, and flows in both at the inlet and outlet in the descending period.

As shown in Figures 7 and 8, the flow rate at the inlet and outlet reaches the peaks in the very beginning of the ascending period and at the very end of the descending period of the piezo disk both for 50 and 90 Hz. Here, the negative value of the flow rate means the fluid flows out of the micropump and the positive value of the flow rate indicates that the fluid flows into the micropump, both at the inlet and outlet. The flow rates have been almost negligible when the descending period

DOI: 10.1002/fld

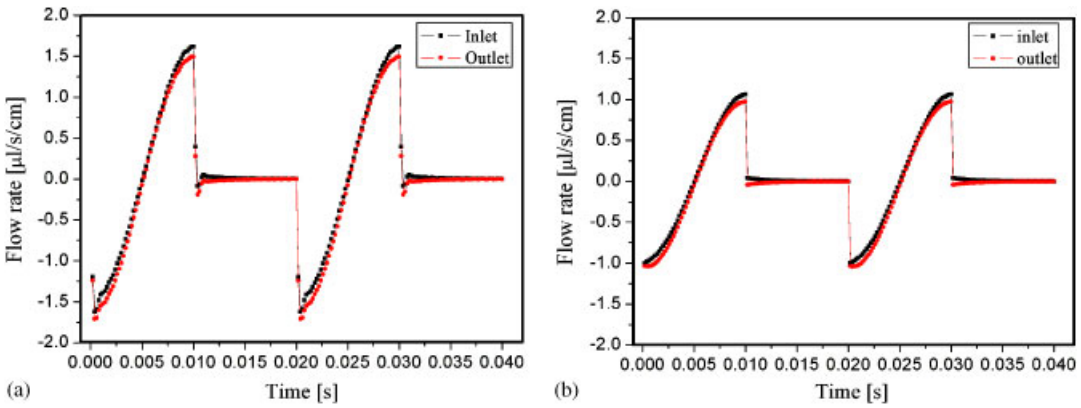

Figure 7. Flow rates at the inlet and outlet with $f = 50$ Hz: (a) FSI model; and (b) prescribed deformation model.

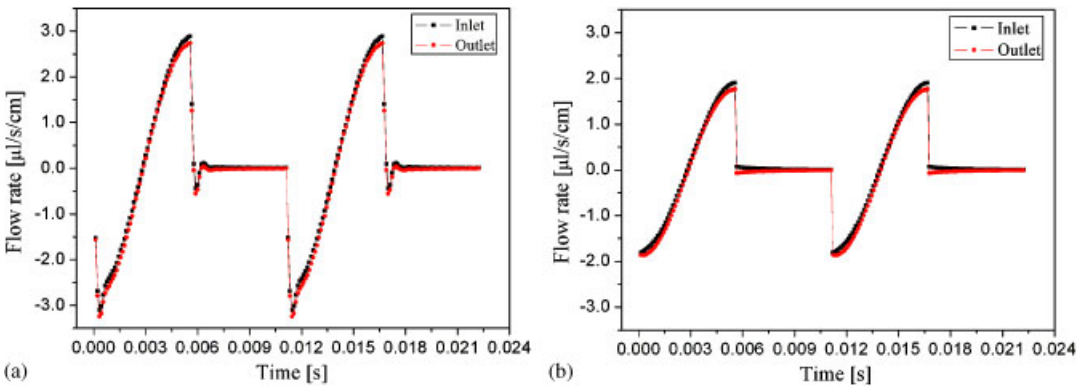

Figure 8. Flow rates at the inlet and outlet with $f = 90$ Hz: (a) FSI model; and (b) prescribed deformation model.

is finished. And the absolute values of flow rate at the inlet and outlet for $f = 90$ Hz are quite larger than those for $f = 50$ Hz. Also, the absolute values of flow rate at the inlet and outlet in the FSI model is larger than those in prescribed deformation model both for 50 and 90 Hz because the space averaged deformation in the FSI model is more considerable than that in the prescribed deformation model. The differences between the inlet and outlet flow rate of the two models have been obtained for 50 and 90 Hz, as shown in Figures 9 and 10 (in association with Figures 7 and 8), respectively. Here again, the difference between the two flow rates of the FSI model is quite larger than that of the prescribed deformation model with $f = 50$ Hz, but this difference is not notable with $f = 90$ Hz. It has been found that the outflow rate at the outlet is larger than that at the inlet in the ascending period and that the inflow rate at the inlet is larger than that at the outlet in the descending period, which yields the net flow from the inlet to the outlet. The net flow rates in the FSI model and the prescribed deformation model are about 2.83 and 2.05 μl/s/cm, respectively,

DOI: 10.1002/fld

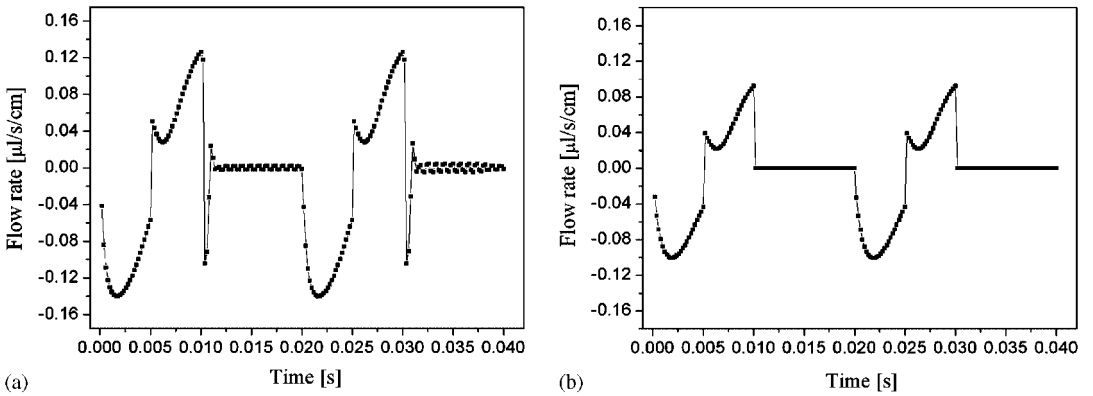

Figure 9. Differences between the inlet flow rate and outlet flow rate with $f = 50$ Hz: (a) FSI model; and (b) prescribed deformation model.

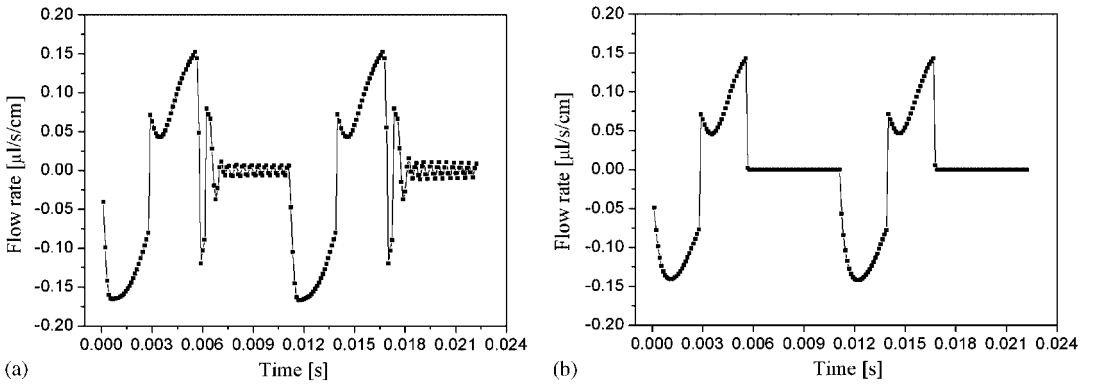

Figure 10. Differences between the inlet flow rate and outlet flow rate with $f = 90$ Hz: (a) FSI model; and (b) prescribed deformation model.

with 50 Hz and those are about 3.76 and 3.61 μl/s/cm, respectively, with 90 Hz. It is clear that these flow characteristics are closely related to the behaviour of the piezo disk or membrane in different numerical models.

When the piezo disk stops finishing the descending, the fluid flow stops immediately in the prescribed deformation model while the fluid flow does not stop immediately but oscillates minutely in the FSI model.

4. CONCLUSION

In this study, a transient numerical analysis using the FSI model and the prescribed deformation model has been conducted for the diffuser-nozzle based piezoelectric micropump. To investigate the effects of the numerical models, the dynamic characteristics of the piezo disk and the flow

DOI: 10.1002/fld

characteristics at the inlet and outlet have been evaluated minutely with time for the frequencies of 50 and 90 Hz.

As a result, the performance characteristics of the FSI model are shown to be a little bit different from those of the prescribed deformation model. Namely, the deformation of the piezo disk in the FSI model is somewhat flat in the central part of the piezo disk, which yields larger net flow rate compared with the prescribed deformation model both for 50 and 90 Hz. And, the net flow rate for 90 Hz is larger than that for 50 Hz both in the FSI model and the prescribed deformation model. Also, for the FSI model when the descending period is finished, the piezo disk does not stop immediately but oscillates minutely.

For a diffuser-nozzle based micropump with a given geometry, both in the FSI model and in the prescribed deformation model, it is expected that there exists an optimal frequency that would yield the maximum net flow rate in a flow channel with given flow resistance.

The results of the present study imply that the choice of numerical model is very important to evaluate the performance characteristics of the diffuser-nozzle based piezoelectric micropump. Also, these results can be utilized as basic data in the design and analysis process of the diffuser/nozzle based piezoelectric micropumps.

ACKNOWLEDGEMENTS

This work was supported by Korea Research Foundation Grant (KRF-2004-041-D00119).

REFERENCES

1. Chang JK, Chung S, Han DC. Application of bio-MEMS technology on medicine and biology. *Journal of the Korean Society of Precision Engineering* 2000; **17**:45–51.
2. Lee SW, Yang SS. Fabrication and applications of micropumps. *ICASE* 1998; 26–32.
3. Stemme E, Stemme G. A valveless diffuser/nozzle-based fluid pump. *Sensors and Actuators A* 1993; **39**:159–167.
4. Schulte S, Maurer A, Bungartz H. *Simulation and Design of Microsystems and Microstructures*. Computational Mechanics Publications: Southampton, 1995; 201–210.
5. Olsson A, Stemme G, Stemme E. Numerical and experimental studies of flat-walled diffuser elements for valve-less micropumps. *Sensors and Actuators A* 2000; **84**:165–175.
6. Anderson H, van der Wijngaart W, Nilsson P, Enoksson P, Stemme G. A valve-less diffuser micropump for microfluidic analytical systems. *Sensors and Actuators B* 2001; **72**:259–265.
7. Nguyen NT, Huang XY. Numerical simulation of pulse-width-modulated micropumps with diffuser/nozzle elements. Nanyang Technological University, 2000.
8. Nguyen NT, Huang XY. Miniature valveless pumps based on printed circuit board technique. *Sensors and Actuators A* 2001; **88**:104–111.
9. Timoshenko S, Woinosky-Krieger S. *Theory of Plates and Shells* (3rd edn). McGraw-Hill: New York, 1959.
10. Song YS. Numerical simulation of flow in a piezoelectric diffuser/nozzle-based micropump for microfluidic application. *MS thesis*, KAIST, Daejeun, Korea, 2002.

DOI: 10.1002/fld